

Article

Mechanical Characterization and Microstructural Analysis of Stir-Cast Aluminum Matrix Composites (LM5/ZrO₂)

Jayavelu Udaya Prakash ¹, Sunder Jebarose Juliyana ¹, Sachin Salunkhe ^{1,*}, Sharad Ramdas Gawade ², Emad S. Abouel Nasr ³ and Ali K. Kamrani ⁴

¹ Department of Mechanical Engineering, Vel Tech Rangarajan Dr. Sagunthala R&D Institute of Science and Technology, Chennai 600062, India; udayaprakashj@veltech.edu.in (J.U.P.); jebarose@veltech.edu.in (S.J.J.)

² Sharadchandra Pawar, College of Engineering and Technology, Someshwar, Baramati 412306, India; s_g212001@yahoo.com

³ Industrial Engineering Department, College of Engineering, King Saud University, P.O. Box 800, Riyadh 11421, Saudi Arabia; eabdelghany@ksu.edu.sa

⁴ Department of Industrial Engineering, Cullen College of Engineering, University of Houston, Houston, TX 77204, USA; akamrani@uh.edu

* Correspondence: drsalunkhesachin@veltech.edu.in

Abstract: Aluminum matrix composites (AMCs) are largely used in defense, maritime, and space applications for their excellent properties. LM5 is used where very high resistance to corrosion from seawater or marine atmospheres is required, for equipment used for the manufacture of foodstuffs, cooking utensils, and chemical plants. Zirconia is preferred over other reinforcements as it shows comparatively great refractory properties, high scratch resistance, and thermal shock resistance. Utilizing the stir casting technique, an attempt was made to produce AMCs of LM5 aluminum alloy strengthened with ZrO₂. The weight percentage of ZrO₂ was changed to 0%, 3%, 6%, and 9%. The specimens were prepared and tested as per ASTM standards to find the density, micro and macro hardness, impact, tensile, and compressive strength. The micrographs and SEM images confirm the uniform distribution of ZrO₂ particles in the aluminum matrix. LM5/9%ZrO₂ AMC has the highest density value of 2.83 g/cm³ and LM5/3%ZrO₂ has the least porosity of 2.55%. LM5/9% ZrO₂ has the highest hardness values of 78 VHN and 72 HRE. LM5/6% ZrO₂ AMC has the highest tensile strength of 220 MPa, compressive strength of 296 MPa, and toughness of 12 J. LM5/6% ZrO₂ AMCs may be used for many structural applications.

Keywords: aluminum matrix composites; impact test; microstructure; stir casting; tensile test; zirconia



Citation: Prakash, J.U.; Jebarose Juliyana, S.; Salunkhe, S.; Gawade, S.R.; Nasr, E.S.A.; Kamrani, A.K. Mechanical Characterization and Microstructural Analysis of Stir-Cast Aluminum Matrix Composites (LM5/ZrO₂). *Crystals* **2023**, *13*, 1220. <https://doi.org/10.3390/cryst13081220>

Academic Editor: Sanbao Lin

Received: 30 June 2023

Revised: 24 July 2023

Accepted: 3 August 2023

Published: 7 August 2023



Copyright: © 2023 by the authors. Licensee MDPI, Basel, Switzerland. This article is an open access article distributed under the terms and conditions of the Creative Commons Attribution (CC BY) license (<https://creativecommons.org/licenses/by/4.0/>).

1. Introduction

In this new era, aluminum is one of the most attractive materials of higher importance, having wider applications in the automobile, construction, electrical, public transport, and aerospace industries. Since conventional construction materials are monolithic, composite materials meet the necessities of such applications. Composites consist of two or more distinct phases, with the additional phase contributing to desired performance characteristics such as rigidity, strength, durability, and self-lubrication. The essential properties of composites are extreme strength, extraordinary thermal conductivity, very high rigidity, low density, oxidation resistance, improved strength-to-weight ratio, and enhanced mechanical properties [1,2].

For many researchers, aluminum metal matrix composites were of interest since the aluminum alloy overwhelms the weaknesses of ferrous materials and offers the preferred specific performance characteristics. Because of its superior resistance to corrosion, light weight, and lower cost compared to other materials, aluminum alloys are still employed as structural materials in ship building and aircraft industries today [3]. MMCs combine the properties of alloys (toughness and ductility) with refractory reinforcement (extraordinary

strength and high modulus) and result in sophisticated service temperature competencies, higher strength, and compression [4,5]. Light weight is the first prerequisite for using AMCs in many sectors. It also provides a remarkable increase in strength. In addition, silicon carbide and boron carbides may be used to modify the thermal expansion coefficient of AMCs [6].

Aluminum alloy has an extreme strength-to-weight ratio, better ductility, and high corrosion resistance [7]. AMCs are manufactured using different practices, such as spray forming, liquid metallurgy, diffusion bonding, and powder metallurgy. The powder metallurgy route is less cost effective than the liquid metallurgy route [8,9]. The main problem with the liquid metallurgy technique is obtaining adequate particle wetting by the molten metal and consistent spreading of the ceramic particles [10]. The unsatisfactory casting technique reported many physical imperfections, such as oxide inclusions, porosity, and particle clustering [11]. The thixotropic behavior, particle formation, and particle distribution of metal matrix composites may be studied.

To determine the effect of stir casting process parameters on homogeneous distribution of reinforcement material in the metal, AMCs were produced using different melting temperatures and holding times. The resulting mechanical properties depend on the cooling rate and the stirring speed used, which depend on the pouring temperature [12,13]. These parameters influence particle dispersal within the matrix. The cluster diameter appeared smaller at a low stirring rate than at a higher stirring rate [14,15]. It has been noted that the hardness is increased through adding reinforcements like fly ash and zirconia with aluminum [16]. A relatively unique aluminum alloy, LM5, is chosen for producing and characterizing composites with a comprehensive literature review [17,18].

Earlier research did not deal with the combination of zirconia and LM5; this composite itself is new. LM5/ZrO₂ composites were fabricated for testing and evaluation. LM5 alloys need more attention in preparation and casting than alloys containing less magnesium because they are more sensitive to oxygen, lubricants, and atmosphere-like moisture. LM5 alloys lack fluidity and appear hot short [19].

In the present work, a novel composite is fabricated through combining LM5 aluminum alloy reinforced with a varying weight percentage of zirconium dioxide using the stir casting method. Mechanical properties like hardness, impact strength, tensile strength, and the microstructure of the fabricated novel composite were evaluated. The motivation behind choosing LM5 aluminum alloy is its excellent corrosion resistance; it can be used in marine applications. So, the authors produced and characterized the composites to find their suitability.

2. Materials Used

2.1. Aluminum Alloy (LM5)

Due to its wide availability and common usage in high-temperature applications, LM5 aluminum is chosen as the matrix metal. The alloy is used for utensils, culinary dishes, chemical industries, and for making castings which need good surface finish, where very much durability against corrosion from sea water or coastal atmospheres is required. LM5 is renowned for its use in industrial, marine plumbing fixtures, structural, and aesthetic maritime gears. The chemical composition of LM5 aluminum alloy was determined through chemical analysis, and the results are presented in Table 1.

Table 1. Chemical composition of LM5 aluminum alloy.

Cu	Mg	Si	Mn	Fe	Pb	Zn	Al
0.032	3.299	0.212	0.022	0.268	0.02	0.01	Balance

2.2. Zirconium Dioxide (ZrO_2)

Zirconium dioxide or zirconia is a commonly studied ceramic material. Zirconia can be extracted using a variety of processes, such as lime fusion, plasma disassociation, and the breakdown of chlorine and alkali oxide. Zirconium dioxide has huge tolerance to the spread of cracks, similar to other ceramic materials. Zirconium dioxide ceramics are thus often thermally produced and are the preferred material for combining ceramics and steel. Zirconium dioxide exhibits desirable properties, such as superior strength and low thermal conductivity [20].

3. Fabrication of LM5/ ZrO_2 Composites

The Remi RQM-122/R agitator system is used in the configuration of the stir casting assembly, which features a C-Type sealed kiln with a power rating of 5 KVA and a suitable temperature range of 500 °C to 1100 °C. The stirrer has a stirring shaft made of SS304 that is 350 mm long, 6 mm in diameter, and includes a socket for simple shaft interchangeability. It comes with a slanted fan-type impeller with four blades that are 38 mm in diameter. The impeller is formed of high chromium steel with high levels of carbon and has been coated with zirconia. Inside the furnace, a silicon carbide crucible is held [21,22].

The LM5 alloy was first charged in a furnace to a temperature of roughly 850 °C till the entire alloy melted there. In a muffle furnace with a 4 KVA output, ZrO_2 is preheated for 20 min to 200 °C in order to remove dampness. The liquid metal is then gradually stirred with ZrO_2 of 70 μ m size at a rate of 600 rpm [23,24]. Magnesium (0.5 wt%) was added to the molten metal to ensure good wettability of ZrO_2 particles with the molten metal. Mg reduces the agglomeration of the ZrO_2 particles and produces sound, defect-free castings [25,26]. For seven minutes, the stirring was continued. Hexachloroethane tablets were used for degassing. Also, argon gas was introduced into the slurry before pouring it into the mold to reduce porosity. The pouring temperature was maintained at 750 °C. The mold was preheated to 650 °C before pouring the slurry into it so that homogeneous solidification could be achieved.

This process produced LM5 alloy and three sets of novel composites consisting of aluminum alloy LM5 reinforced with 3%, 6%, and 9% by weight of ZrO_2 particles [27,28]. The stir casting setup is shown in Figure 1. Figure 2 depicts the fabrication of the LM5 and composites, and the molten mixture is poured into the mold.



Figure 1. Stir casting setup.



Figure 2. Pouring molten mixture into the preheated mold and fabricated composites.

4. Micro Structural Analysis

4.1. Optical Microscopy

Examining the microstructure of aluminum and its composites requires a carefully executed series of steps that depend on theoretical knowledge and professional experience. Generally, sample preparation involves a series of steps: sectioning or cutting, arranging, processing, and polishing. In several cases, cutting is sufficient to obtain a small piece for examination. An inverted optical microscope examined the AMCs. The sample's surfaces are smoothed using sandpaper via mesh sizes ranging from 220 to 1500, and then polished using velvet cloth. Each composite specimen was meticulously polished to match the surface's texture [29]. The specimens were then etched using HF solution prior to microscopic examination. Metallographic analyses provide beneficial information for fabricating good-quality composites.

Microstructure is the very-small-scale structure of a material, defined as the structure of a prepared material surface as revealed using an optical microscope. Crystalline lattice materials (composites, metals, ceramics, and polymers) may significantly impact physical properties like resilience, strength, ductility, stiffness, corrosion protection, etc. Those properties also regulate the usage of such materials in industrial applications. Numerous faults in the structure might either be present or not, which impacts the microstructure's role in a material's physical and mechanical properties. Although these faults can take many shapes, pores are the most common. These pores ultimately determine the features of materials and their formulation. Additionally, different phases may exist in some materials at the same time. If properly handled, these phases may have a variety of characteristics and stop the material from breaking [30].

4.2. Scanning Electron Microscopy (SEM & EDAX)

Microstructure analysis has become one of the methods to study alloys, and composite materials to ascertain the results of different products and measure the effects of new techniques, the cause of errors, and evaluate them. Microstructure analysis is typically performed to assess the material response to thermal processing. The chosen microstructure of metal and non-metal is formed or altered through heat treatment production. A "fingerprint" of processing can be seen in the crystal structure of materials.

AMCs' microstructure is studied to confirm the uniform distribution of the reinforcement. SEM offers numerous advantages, including easy handling of specimens, the largest magnification scale (often between 15 to 50,000 times), and the ability to see significant portions of the specimen's outer layer, including the origin and spread zones. It is possible to focus on surfaces with broad topographies through placing the surface directly into the microscope because of its superior field depth [31]. EDAX is an energy-dispersive X-ray spectroscopy (EDS) technique used for elemental analysis [32].

5. Mechanical Characterization

5.1. Density

Density is the physical property that reflects the characteristics of composites. Experimentally, the density of a composite is obtained via displacement techniques using a physical balance with a density measuring kit as per the ASTM: D 792-66 test method. The mass of a specimen is measured using an electronic weighing machine with 0.001 g accuracy. The volume of a specimen is measured through measuring the water displacement using a graduated cylinder. First, the water level of the graduated cylinder is noted, and then the test specimen is immersed in it. The difference in water level is measured; it is the volume of the specimen. Density was determined using the formula mass/volume. Porosity measures a material's volume (or amount) of space about its overall size [33]. Utilizing the formula, it is calculated as shown in Equation (1).

$$\text{Porosity}\% = (1 - D_e/D_t) \times 100 \quad (1)$$

where D_e is the experimental density; D_t is the theoretical density.

5.2. Micro Hardness

The Vickers hardness test (ASTM E384) is commonly used to assess the micro hardness of materials. The hardness value is mentioned in VHN (Vickers Hardness Number). Micro hardness tests can gather the information required to measure distinct microstructures into a larger matrix, analyze excellent foils like plastics, or determine the hardness gradient along a specimen's transverse. It uses loads < 1 kgf. An apical angle diamond with 136° is used in the Vickers Hardness Test. Typically, the surface that will be evaluated requires a highly polished surface. A higher metallographic polish is obtained with the little force that is used. Direct measurement of the contoured indents requires a microscope with $500\times$ magnification.

5.3. Macro Hardness

The indentation hardness of the substrate serves as the basis for the Rockwell scale. The Rockwell hardness test (ASTM E18) is used to quantify hardness. The Rockwell hardness of the material can be determined through first applying a light load and then a heavy force. An outcome is a dimensionless number presented as HRA, HRB, HRC, HRE, etc., where the Rockwell scale is indicated by the letter before it based on the different indenters or weights used. The hardness of as-cast composites and the unreinforced alloy was measured using Rockwell hardness test scale E (1/8-inch steel ball with a minor load of 10 kgf and a major load of 90 kgf). The samples were first surface finished, and at least five measurements were performed randomly in each sample and averaged to obtain the accurate hardness of the specimen [34].

5.4. Tensile Strength

The fabricated composite materials were evaluated using a computerized Universal Testing Machine (UTM). The tensile test was conducted at ambient temperature following the ASTM E8 standard. The results of the tensile test are taken into consideration while choosing engineering materials. Tensile qualities must be included in the material specifications to guarantee performance. To compare various materials and methods, tensile properties are measured when producing new materials and processes. Eventually, the tensile characteristics are used to assess a material's behavior under conditions apart from uniaxial stress charging [35,36]. The stress required for significant plastic deformation or the maximum stress a material can withstand can be used to gauge a material's strength, which is always the main issue. Another issue is the material's toughness, which measures how far it can bend before breaking. Ductility is the ability of a material to plastically deform without breaking when tensile stress is applied to it. Elastic properties can also be of concern. Universal testers are the most popular testing machines which measure materials' response to stress, compression, or bending [37].

5.5. Compressive Strength

The fabricated composites were tested for compressive strength using a computerized UTM following ASTM E8 standards. Numerous fields require compressive tests. Engineering materials are chosen using the results of the compressive test. The material specifications must provide compressive qualities to assure performance. Compressive Test properties are measured when producing new materials and processes to compare various materials and methods. Ultimately, the compressive Test characteristics are used to assess a material's behavior under conditions apart from uniaxial stress charging. Universal testers are the most popular testing machines which measure materials in stress, compression, or bending [38].

5.6. Impact Strength

Impact strength refers to a material's capacity to endure an applied force or a rapid load. It is presented as energy lost per unit of area in square meters (J/m^2). The Izod impact test is a common ASTM method (ASTM E23) for evaluating the toughness of a material. The Izod impact test involves striking a sample with a swinging arm of known energy. The sample is fixed in a cantilever beam. A pivoting arm is raised to a specific height (constant potential energy) and then released. The arm swings down, hitting a notched sample, breaking the specimen. The energy absorbed by the sample is calculated from the height the arm swings to after hitting the sample [39].

6. Results and Discussions

6.1. Microstructural Analysis

The optical micrographs show how evenly the zirconia particles have dispersed throughout the matrix. Particles in the order of distribution start to coagulate and disturb homogeneity as the wt% of the reinforcement rises. The AMCs strength is provided by uniform reinforcement spread, which is the primary reason for improved mechanical characteristics [40,41]. Figure 3 shows the microstructure of LM5 and all the fabricated composites at 100 times magnification.

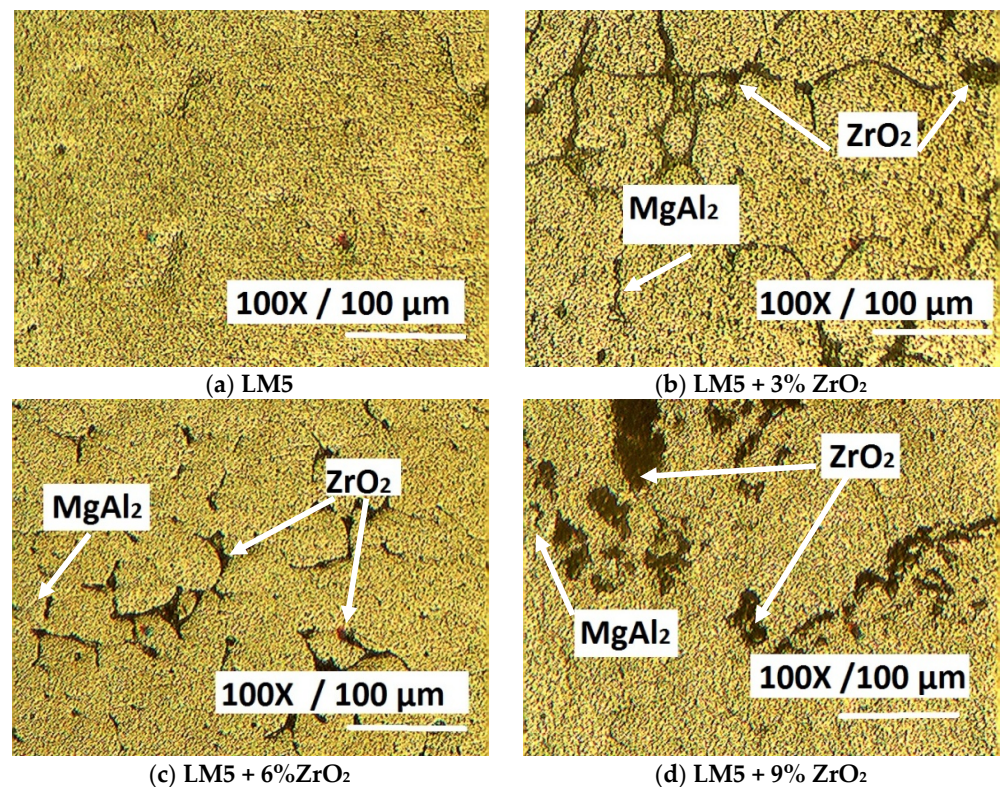


Figure 3. Micrographs of LM5 alloy and LM5/ZrO₂ composites.

The microstructure of LM5 shows an interdendritic pattern of aluminum. The grain borders are precipitated with $MgAl_2$ eutectic particles, which were not dissolved during solidification [42].

The primary aluminum phase grain size is measured as 40 to 50 microns. The precipitated eutectic $MgAl_2$ particles are present in the primary aluminum grains. The microstructures of AMCs with 3% and 6% ZrO_2 show a uniform distribution of ZrO_2 . The particles are embedded in the aluminum grains. A ZrO_2 particle distribution of 9% is present as clusters along the grain boundaries [43]. During this research, ZrO_2 is introduced to the aluminum alloy LM5 as reinforcement to evaluate the transition in AMC properties. The work aims to examine the impact of reinforcement (zirconia) on castability as part of the larger initiative to enhance the efficiency of cast aluminum LM5. Figure 4 displays the SEM pictures of LM5 Al alloy and AMCs (LM5/ ZrO_2). It is clear from these SEM images that particles scattering within the matrix were uniform. At lower magnifications, scanning electron micrographs show uniform ceramic particle dispersion in the AMCs, while at greater sizes; the SEM shows matrix–particle interfaces.

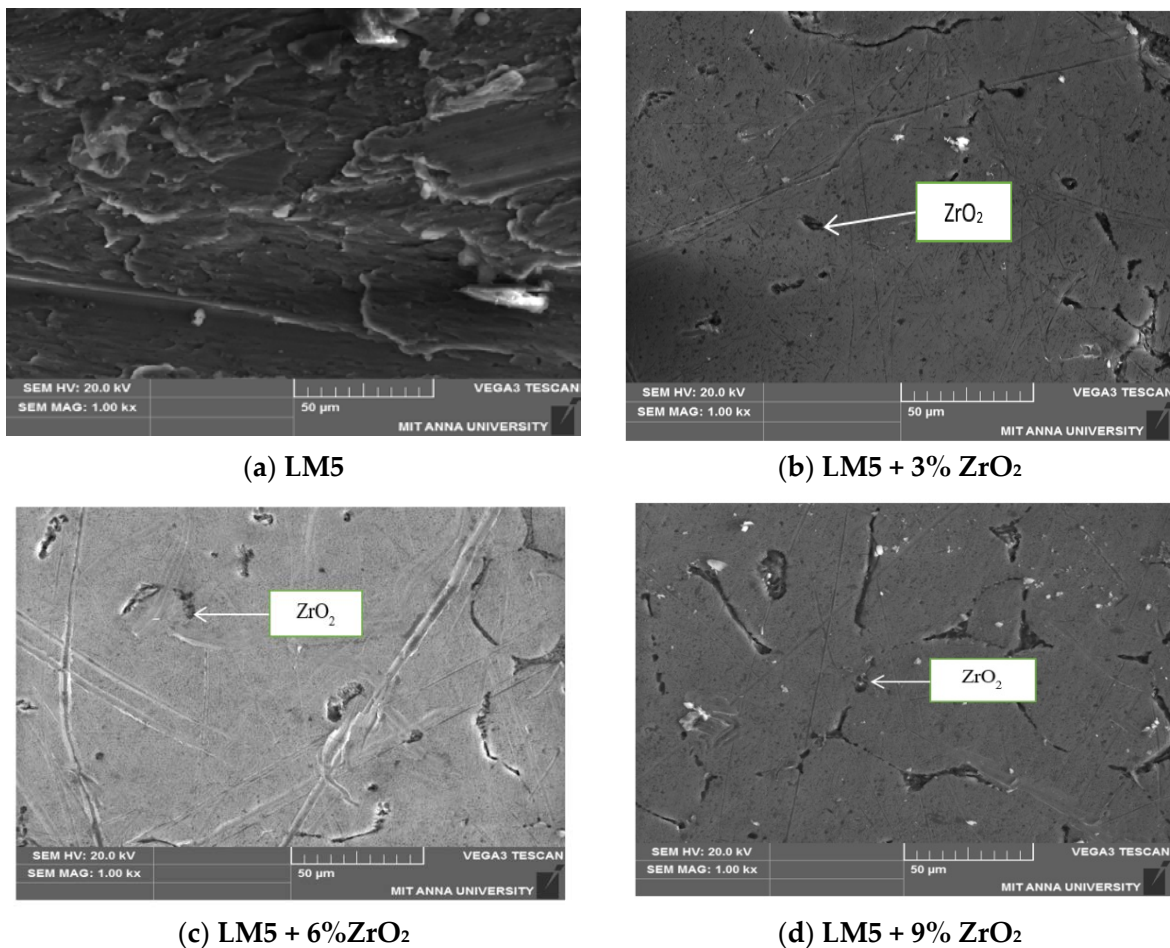


Figure 4. SEM images of LM5 and LM5/ ZrO_2 composites.

The SEM images demonstrate the homogeneous distribution of reinforced ZrO_2 particles within the aluminum alloy matrix. These figures illustrate the homogeneity of composite materials in comparison. Scanning electron micrographs test the relationship between particle distribution and Zirconia weight fraction. The wettability improved since no pores were discovered in either situation. This interfacial bonding was achieved because of too-quick cooling. The area fraction increases with the increase in the wt% of ZrO_2 . It is also observed that the ZrO_2 reinforcement weight percentage increases while the average grain size of the Aluminum LM5 matrix decreases.

It is also believed that the increase in the interfacial bonding of the reinforcement with the aluminum matrix alloy is responsible for increased mechanical characteristics. This is due to ZrO_2 's high specific gravity, which is consistent with the efficient selection of stirring settings and full wetting of warmed ZrO_2 particles prior to application to the matrix alloy. When primary and structural information is needed for micro- and nano-characterization, EDAX creates the optimum solutions, enhancing the usability and precision of analysis. Figure 5 displays the EDAX of composites made of LM5, ZrO_2 , and LM5. EDAX confirms the presence of ZrO_2 and graphite particles scattered in composites.

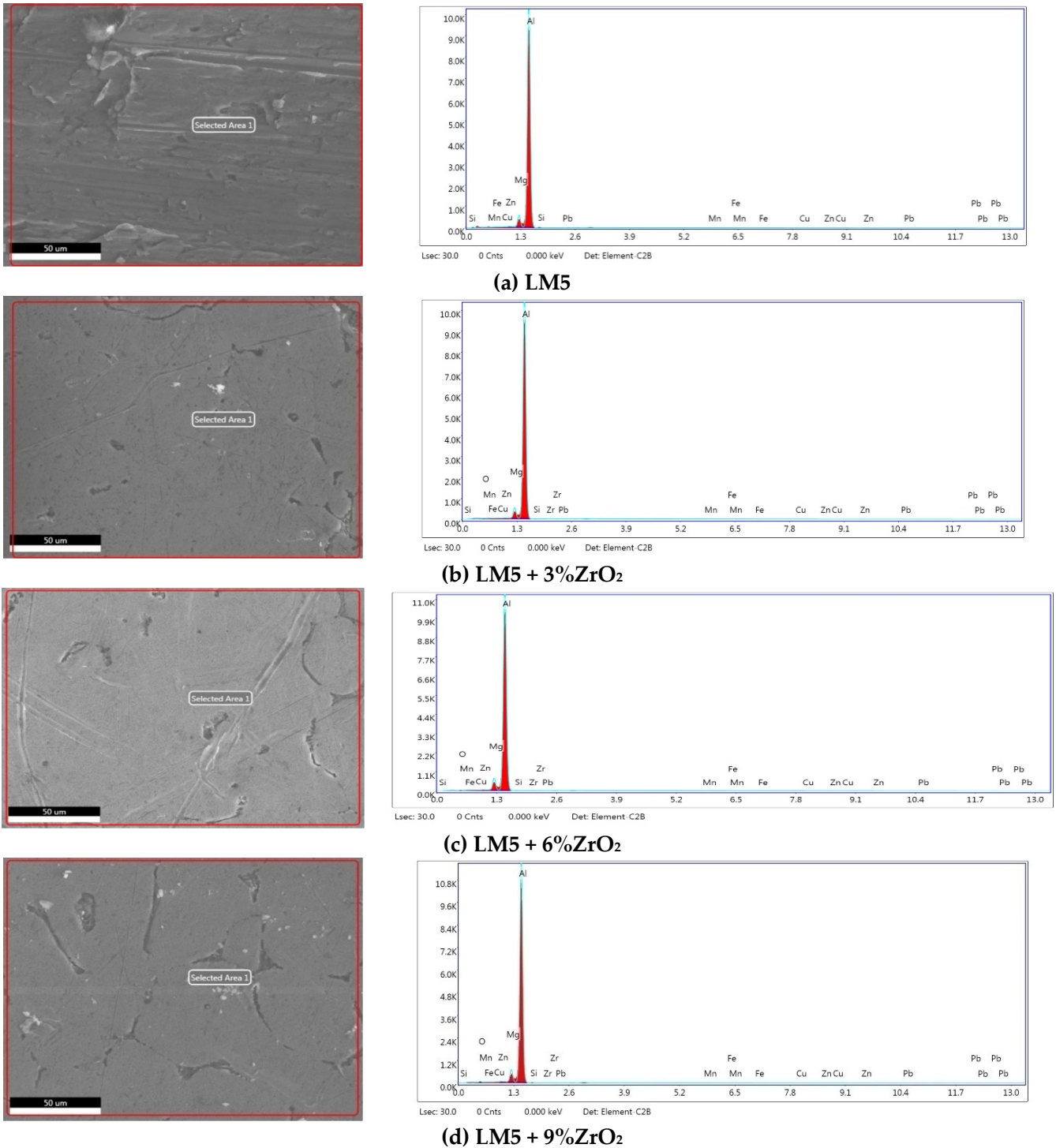


Figure 5. EDAX of LM5 and LM5/ ZrO_2 Composites.

6.2. Density

The mass of the cast composites is determined using an electronic weighing instrument with a precision of 0.001 g. The volume of the composites is calculated through immersing the composites into the graduated cylinder and measuring the displacement of water [44]. The D_e (experimental density) and D_t (theoretical density) of the cast plain LM5 aluminum alloy is 2.61 and 2.65 g/cm³, respectively, and both densities of all the novel fabricated composites are slightly more than LM5 plain aluminum alloy. The higher densities of the composites result from the inclusion of ZrO₂, which has a 5.68 g/cm³ density. The porosity of the produced composites slightly increases since eutectic alloys tend to form large pores through increasing the weight percentage of the reinforcement. Figures 6 and 7 display the effect of ZrO₂ on the density and porosity of AMCs.

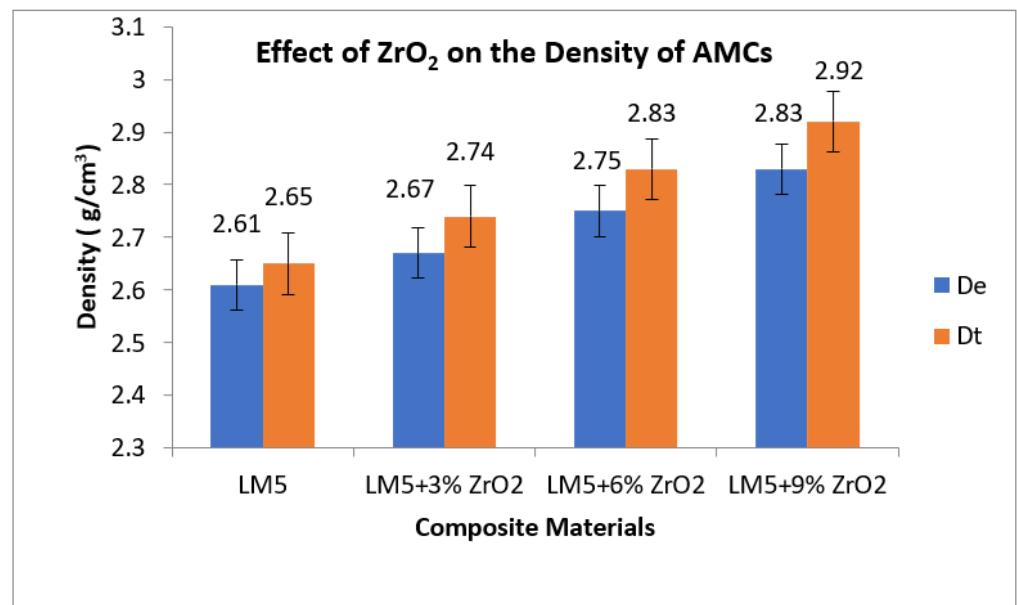


Figure 6. Effect of ZrO₂ on the density of AMCs.

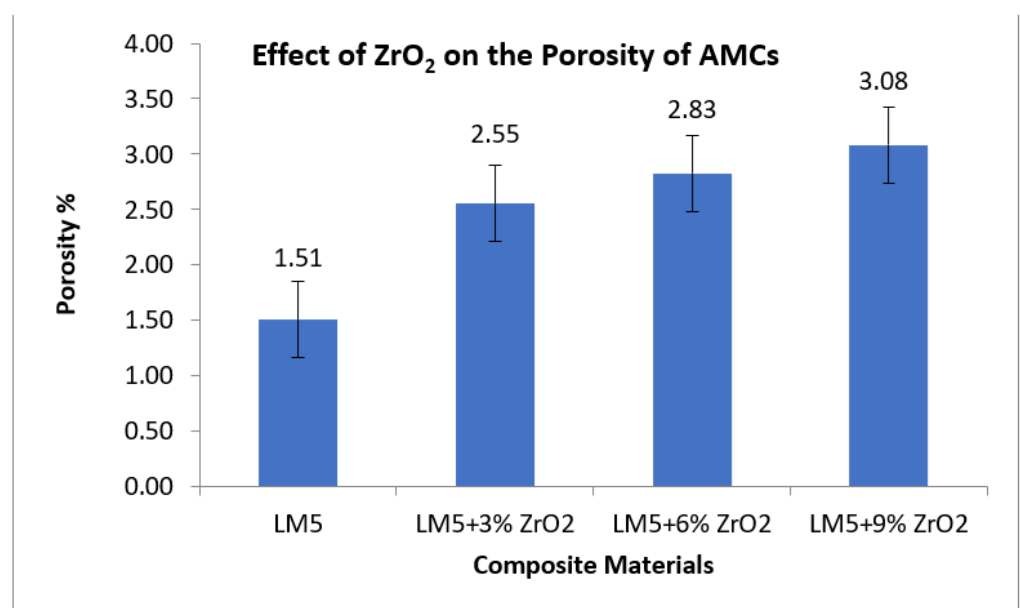


Figure 7. Effect of ZrO₂ on the porosity of AMCs.

6.3. Micro Hardness

Figure 8 depicts how ZrO_2 affects the hardness of AMCs. LM5 + 9% ZrO_2 have the highest hardness of 78 VHN. The introduction of ZrO_2 with a metal matrix increases the hardness value. Reinforcement strengthens the metal matrix during composite processing, and the unique hardness properties of ZrO_2 are passed to the specimen. Figure 8 shows that the hardness is directly proportional to the addition of the ceramic reinforcement. The presence of rigid particles increases the resistance to plastic deformation, resulting in higher composite hardness. The total area of the reinforcements increases when reinforcing particles are added to composites [45].

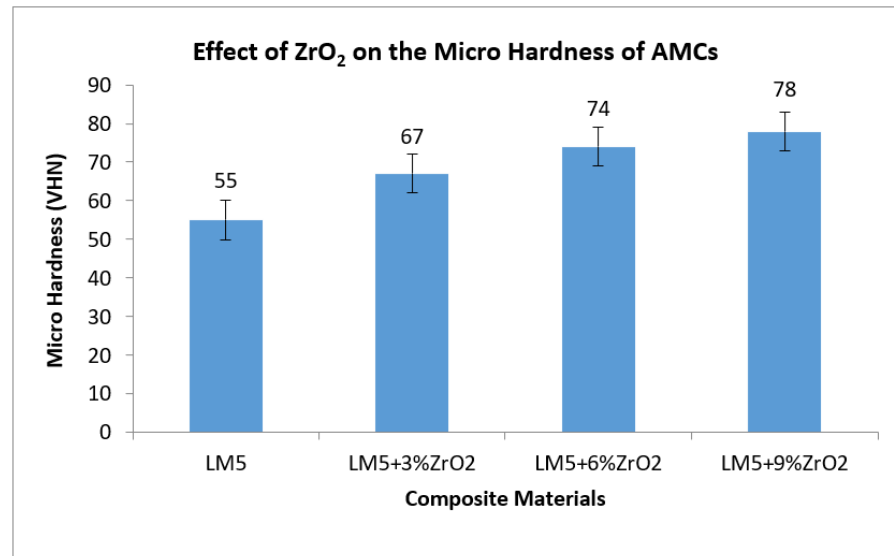


Figure 8. Effect of ZrO_2 on the micro hardness of AMCs.

6.4. Macro Hardness

The effect of ZrO_2 on the hardness is shown in Figure 9. The Rockwell hardness value of LM5 alloy is found to be 41 HRE. The hardness value increased drastically to 57 HRE, 67 HRE, and 72 HRE, respectively, for 3% ZrO_2 , 6% ZrO_2 , and 9% ZrO_2 . The presence of hard particles makes plastic distortion more opposed, contributing to increased material hardness. The total area of the reinforcements increases via applying the reinforcing particles to the composites [46].

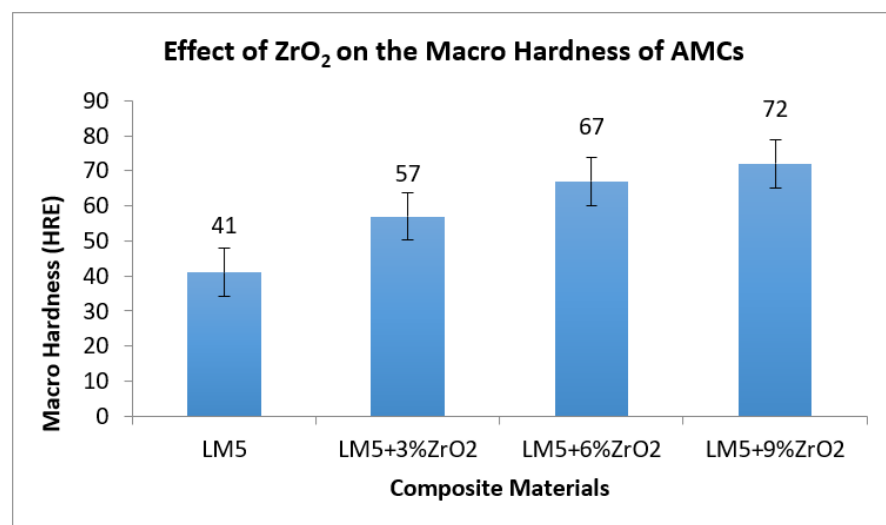


Figure 9. Effect of ZrO_2 on the macro hardness of AMCs.

6.5. Tensile Strength

The tensile test reveals that when the wt% of the particulates in ZrO_2 rises, so does the strength of the LM5/ ZrO_2 composites. The impact of zirconium dioxide weight percentage on the composite tensile strength of aluminum alloy LM5 and ZrO_2 is depicted in Figure 10. The composition of zirconia is monoclinic, whereas the composition of aluminum crystallizes in FCC. It is irrational to say that the various crystalline structures of zirconia and aluminum cause their interaction.

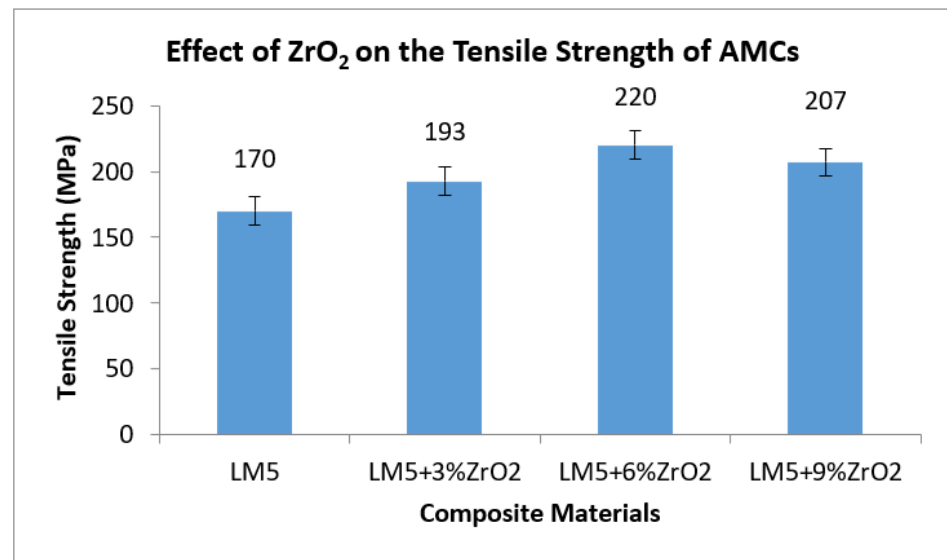


Figure 10. Effect of ZrO_2 on the tensile strength of AMCs.

Therefore, this incoherence boosts the AMCs' strength. The high stiffness rate of the AMCs during their strain is likely the cause of the elevated hardness of the aluminum. The elastic characteristics of ZrO_2 particles and ability to resist matrix deformation might enhance their hardening function. Thus, the ZrO_2 particles promote work hardening and inhibit matrix deformation in the presence of a suitable contact. The tension created by the unique coefficient of thermal expansion of zirconia ($10 \times 10^{-6} K^{-1}$) and aluminum ($16 \times 10^{-6} K^{-1}$) can also increase the number of dislocations and, consequently, the composite strength is increased. Dislocation movement is hampered via accumulating behind ZrO_2 particles and increasing dislocation density. The number of dislocations generated increases with the increasing amount of ZrO_2 [47].

The LM5 alloy, in its purest form, has a tensile strength of 170 MPa. The ZrO_2 particles, according to the results, significantly boost the tensile strength of the aluminum alloy composite. The tensile strength of AMCs made of aluminum alloy with 3% ZrO_2 is 193 MPa, increasing to 220 MPa with 6% ZrO_2 and decreasing to 207 MPa with LM5 + 9 wt% ZrO_2 . It is evident from the findings of the study that the composites' tensile strength is increased when compared to the LM5 aluminum alloy. The impact of zirconium dioxide on the elongation percentage is depicted in Figure 11. According to the results, the material's elongation diminishes when zirconium dioxide is added in weight percentages. Through adding zirconium dioxide, the LM5 elongates 3.24%, loses its ductility, and turns brittle. Elongation of LM5 + 3% ZrO_2 is observed to be 2.43%; however, this value is decreased to 2.3% and 2.21% for the compositions of LM5 + 6 wt% of ZrO_2 and LM5 + 9% ZrO_2 , respectively. UTS, strain, and elongation for the manufactured composite are smaller for the 9% reinforcement than for the 6% ZrO_2 due to the brittleness of the latter. At 6% ZrO_2 , the greatest ultimate tensile strength is seen. Cluster formations have yet to be observed with 9% reinforcement, which is expected to result in lower mechanical qualities, particularly tensile strength, compared to 6% reinforcement.

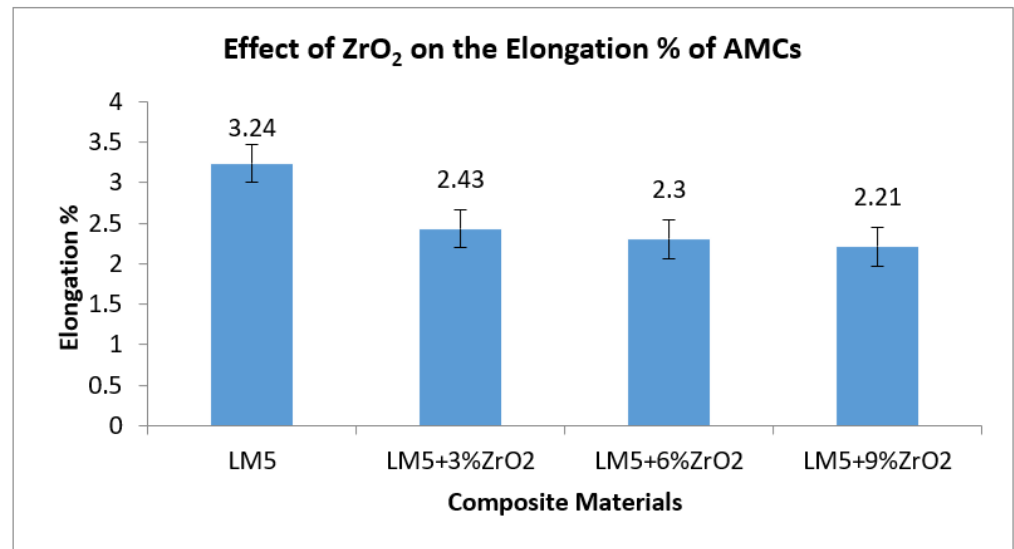


Figure 11. Effect of ZrO₂ on the elongation percentage of AMCs.

6.6. Compression Strength

The LM5 alloy has a compressive strength of 273 MPa. The ZrO₂ particles, according to the results, significantly enhance the compression strength of the AMCs. The AMC reinforced with 3% ZrO₂ has a 277 MPa compressive strength, whereas the alloy with 6% ZrO₂ has a 296 MPa compressive strength. The stress was further decreased to 278 MPa for the mixture of LM5 + 9 wt% ZrO₂. The experimental findings show that the composites' compression strength is greater than the LM5 aluminum alloy. The impact of zirconium dioxide on the compression strength and compression % is depicted in Figures 12 and 13. Results indicate that increasing the wt% of ZrO₂ boosts the AMCs' compression strength [48]. Through adding zirconium dioxide, the LM5, whose compression is 35.9%, loses its ductility and turns brittle instead of ductile. The compression of LM5 + 3% ZrO₂ is observed to be 40.32%; this value increases to 45.32% for LM5 + 6 wt% ZrO₂ and subsequently decreases to 36.3% for LM5 + 9 wt% ZrO₂. At 6% ZrO₂, the greatest compressive strength is seen.

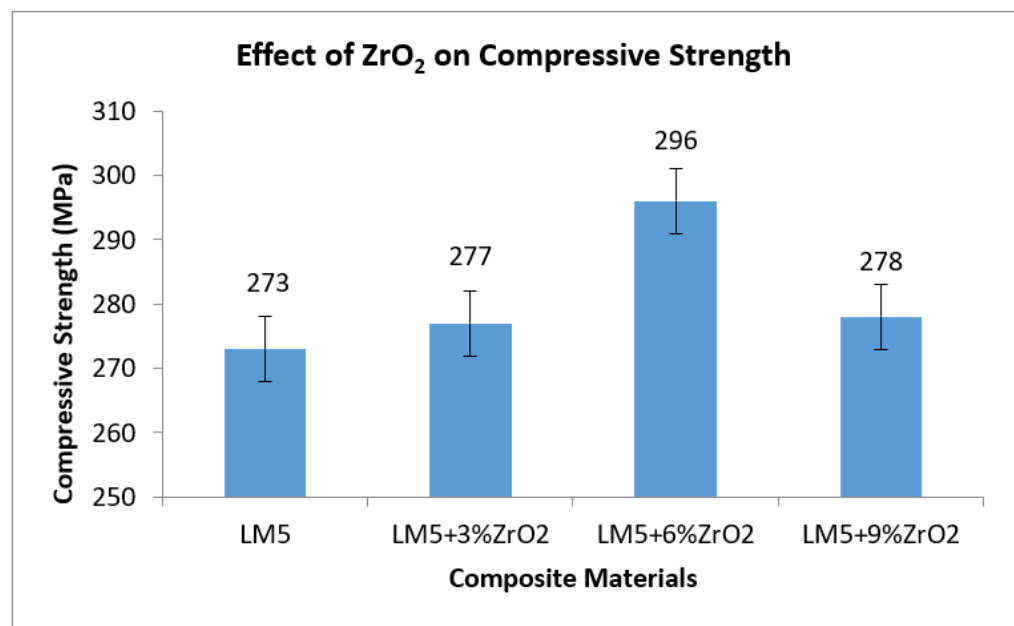


Figure 12. Effect of ZrO₂ on the compression strength of AMCs.

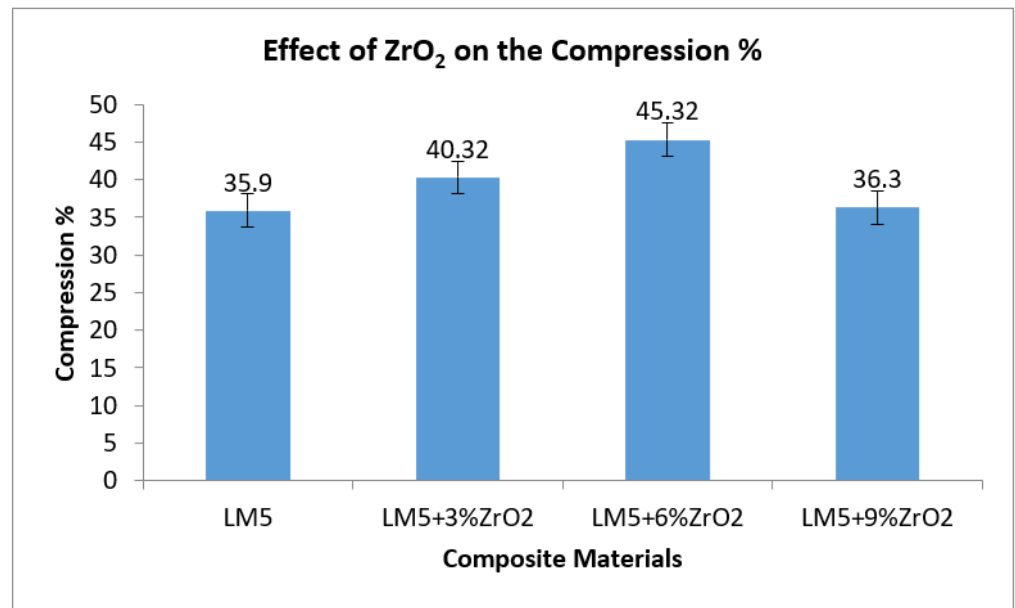


Figure 13. Effect of ZrO₂ on the compression percentage of AMCs.

6.7. Impact Strength

An Izod impact test is used to gauge the produced composite's toughness. Figure 14 demonstrates that the AMCs' toughness increases with an increased wt% of ZrO₂ reinforcement.

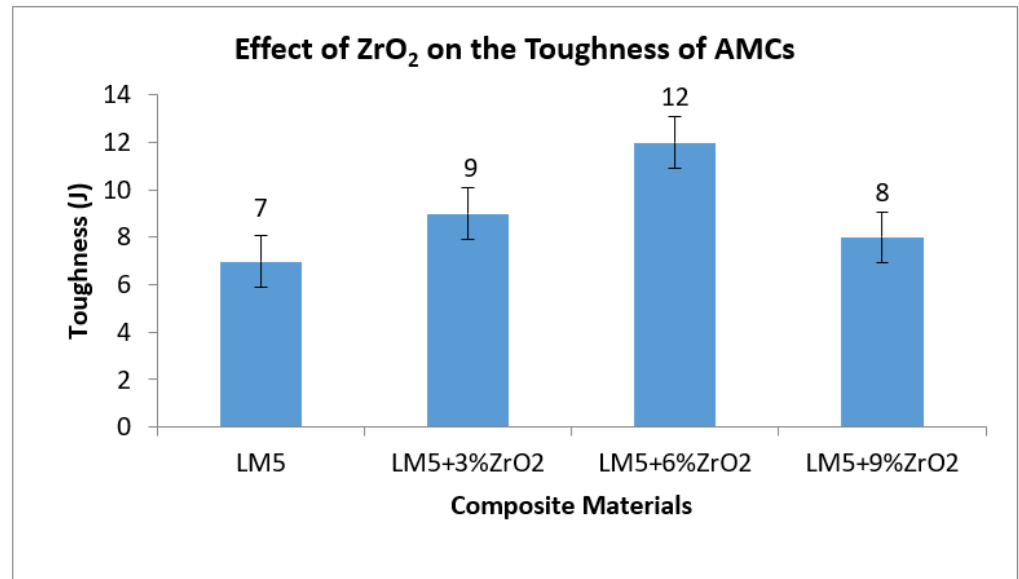


Figure 14. Impact strength of fabricated composites AMCs.

In 6% ZrO₂, the impact strength of plain LM5 increases to 12 Joules from 7 Joules. The strong link that forms between the matrix and the reinforcing ZrO₂ may be the cause of the impact energy increases with reinforcement. Additionally, the reinforcing particle agglomeration feature that creates mesh, a fragile area in the composites, may cause a drop in impact strength over and above six percent reinforcement [49,50]. Nevertheless, the impact strength of all the manufactured AMCs is considerably higher than the impact strength of LM5 aluminum alloy.

7. Conclusions

The stir casting process produced composite metal matrix materials with uniformly dispersed ZrO₂ particles and increased ZrO₂ particle weight, increasing density slightly while enhancing micro and macro hardness. The impact strength, compression, and tensile strength of MMCs were significantly improved through increasing the weight of ZrO₂ particles by up to 6% in the LM5 matrix and decreasing the reinforcement by 9% due to agglomeration. The transition of materials from ductile to brittle reduces the composites' elongation ability, because it has increased mechanical qualities like hardness as well as tensile, compression, and impact strength.

- (i) The optical micrograph and SEM of the AMCs show a uniform distribution of reinforcement particles in the matrix. EDAX shows the presence of constituents.
- (ii) The LM5/9%ZrO₂ AMC has the highest density value of 2.83 g/cm³. The LM5/3%ZrO₂ AMC has a porosity of 2.55%.
- (iii) The LM5/9% ZrO₂ AMC has the highest micro hardness value of 78 VHN and macro hardness of 72 HRE.
- (iv) The LM5/6% ZrO₂ AMC has the highest tensile strength of 220 MPa, highest compressive strength of 296 MPa, and hardest toughness of 12 J.
- (v) The LM5/6% ZrO₂ AMCs may be used for many structural applications due to their excellent mechanical properties.

Author Contributions: Conceptualization, S.J.J. and J.U.P.; methodology, S.S.; formal analysis, J.U.P. and S.J.J.; investigation, E.S.A.N. and A.K.K.; resources, S.J.J.; data curation, S.S. and S.R.G.; writing—original draft preparation, S.J.J.; writing—review and editing, S.S. and J.U.P.; visualization, S.S. and S.R.G.; supervision, J.U.P.; project administration, S.S.; funding acquisition, E.S.A.N. and A.K.K. All authors have read and agreed to the published version of the manuscript.

Funding: King Saud University for funding this work through Researchers Supporting Project number (RSP2023R164), King Saud University, Riyadh, Saudi Arabia.

Data Availability Statement: The data presented in this study are available through email upon request to the corresponding author.

Acknowledgments: The authors extend their appreciation to King Saud University for funding this work through Researchers Supporting Project number (RSP2023R164), King Saud University, Riyadh, Saudi Arabia.

Conflicts of Interest: The authors declare that they have no conflict of interest.

References

1. Shi, Q.; Zhou, J.; Ullah, S.; Yang, X.; Tokarska, K.; Trzebicka, B.; Ta, H.Q.; Rummeli, M.H. A review of recent developments in Si/C composite materials for Li-ion batteries. *Energy Storage Mater.* **2021**, *34*, 735–754. [[CrossRef](#)]
2. Nturanabo, F.; Masu, L.; Kirabira, J.B. *Novel Applications of Aluminium Metal Matrix Composites. Aluminum Alloys and Composites*; IntechOpen: London, UK, 2020. [[CrossRef](#)]
3. Blanco, D.; Rubio, E.M.; Lorente-Pedreille, R.M.; Sáenz-Nuño, M.A. Lightweight Structural Materials in Open Access: Latest Trends. *Materials* **2021**, *14*, 6577. [[CrossRef](#)] [[PubMed](#)]
4. Zhang, C.; Zhu, J.; Ji, C.; Guo, Y.; Fang, R.; Mei, S.; Liu, S. Laser powder bed fusion of high-entropy alloy particle-reinforced stainless steel with enhanced strength, ductility, and corrosion resistance. *Mater. Des.* **2021**, *209*, 109950. [[CrossRef](#)]
5. Prakash, J.U.; Moorthy, T.; Ananth, S. Fabrication and Sliding Wear Behaviour of Metal Matrix Composites. *Appl. Mech. Mater.* **2014**, *612*, 157–162. [[CrossRef](#)]
6. Sadhana, A.D.; Prakash, J.U.; Sivaprakasam, P.; Ananth, S. Wear behaviour of aluminium matrix composites (LM25/Fly ash)—A Taguchi approach. *Mater. Today Proc.* **2020**, *33*, 3093–3096. [[CrossRef](#)]
7. Srikanth, M.; Annamalai, A.R.; Muthuchamy, A.; Jen, C.-P. A Review of the Latest Developments in the Field of Refractory High-Entropy Alloys. *Crystals* **2021**, *11*, 612. [[CrossRef](#)]
8. Ravi, B.; Naik, B.B.; Prakash, J.U. Characterization of Aluminium Matrix Composites (AA6061/B4C) Fabricated by Stir Casting Technique. *Mater. Today Proc.* **2015**, *2*, 2984–2990. [[CrossRef](#)]
9. Danninger, H.; Calderon, R.D.O.; Gierl-Mayer, C. Powder metallurgy and sintered materials. *Addit. Manuf.* **2017**, *19*, 1–57.
10. Meena, K.; Manna, A.; Banwait, S. An Analysis of Mechanical Properties of the Developed Al/SiC-MMC's. *Am. J. Mech. Eng.* **2013**, *1*, 14–19. [[CrossRef](#)]

11. Ravikumar, M.; Reddappa, H.N.; Suresh, R. Study on mechanical and Tribological characterization of Al₂O₃/SiCp reinforced aluminum metal matrix composite. *Silicon* **2018**, *10*, 2535–2545. [[CrossRef](#)]
12. Rino, J.; Sivalingappa, D.; Koti, H.; Jebin, D.V. Properties of Al6063 MMC Reinforced with Zircon Sand and Alumina. *IOSR J. Mech. Civ. Eng.* **2013**, *5*, 72–77. [[CrossRef](#)]
13. Girisha, K.B.; Chittappa, H.C. Preparation, Characterization and Wear Study of Aluminum Alloy (Al 356.1) Reinforced with Zirconium Nano Particles. *Int. J. Innov. Res. Sci. Eng. Technol.* **2013**, *2*, 3627–3637.
14. Nathan, V.B.; Soundararajan, R.; Abraham, C.B.; Vinoth, E.; Narayanan, J. Study of mechanical and metallurgical characterization of correlated aluminium hybrid metal matrix composites. *Mater. Today Proc.* **2021**, *45*, 1237–1242. [[CrossRef](#)]
15. Malhotra, S.; Narayan, R.; Gupta, R.D. Synthesis and Characterization of Aluminum 6061 Alloy-Fly ash & Zirconia Metal Matrix Composite. *Int. J. Curr. Eng. Technol.* **2013**, *3*, 1716–1719.
16. Madhusudhan, M.; Naveen, G.; Mahesha, K. Mechanical Characterization of AA7068-ZrO₂ reinforced Metal Matrix Composites. *Mater. Today Proc.* **2017**, *4*, 3122–3130. [[CrossRef](#)]
17. Jebarose Juliyana, S.; Udaya Prakash, J.; Čep, R.; Karthik, K. Multi-Objective Optimization of Machining Parameters for Drilling LM5/ZrO₂ Composites Using Grey Relational Analysis. *Materials* **2023**, *16*, 3615. [[CrossRef](#)]
18. Jebarose Juliyana, S.; Udaya Prakash, J.; Salunkhe, S. Optimisation of wire EDM process parameters using Taguchi technique for machining of hybrid composites. *Int. J. Mater. Eng. Innov.* **2022**, *13*, 257–271. [[CrossRef](#)]
19. Rubi, C.S.; Prakash, J.U. Drilling of Hybrid Aluminum Matrix Composites using Grey-Taguchi Method. *INCAS Bull.* **2020**, *12*, 167–174. [[CrossRef](#)]
20. Jebarose Juliyana, S.; Udaya Prakash, J. Optimization of Machining Parameters for Wire EDM of AMCs (LM5/ZrO₂) using Taguchi Technique. *INCAS Bulletin* **2022**, *14*, 57–68. [[CrossRef](#)]
21. Zhang, W.Y.; Du, Y.H.; Zhang, P.; Wang, Y.J. Air-isolated stir casting of homogeneous Al-SiC composite with no air entrapment and Al₄C₃. *J. Mater. Process. Technol.* **2019**, *271*, 226–236. [[CrossRef](#)]
22. Sozhamannan, G.G.; Prabu, S.B.; Venkatagalapathy, V.S.K. Effect of Processing Parameters on Metal Matrix Composites: Stir Casting Process. *J. Surf. Eng. Mater. Adv. Technol.* **2012**, *2*, 11–15. [[CrossRef](#)]
23. Ahmed, M.M.Z.; Essa, A.R.S.; Ataya, S.; Seleman, M.M.E.-S.; El-Aty, A.A.; Alzahrani, B.; Touileb, K.; Bakkar, A.; Ponnore, J.J.; Mohamed, A.Y.A. Friction Stir Welding of AA5754-H24: Impact of Tool Pin Eccentricity and Welding Speed on Grain Structure, Crystallographic Texture, and Mechanical Properties. *Materials* **2023**, *16*, 2031. [[CrossRef](#)]
24. Ghiasvand, A.; Ranjbarnodeh, E.; Mirsalehi, S.E. The microstructure and mechanical properties of single-pass and double-pass lap joint of Al 5754H-11 and Mg AZ31-O alloys by friction stir welding. *J. Mater. Res. Technol.* **2023**, *23*, 6023–6038. [[CrossRef](#)]
25. Bhandare, R.G.; Sonawane, P.M. Preparation of aluminium matrix composite by using stir casting method. *Int. J. Eng. Adv. Technol.* **2013**, *3*, 61–65.
26. Jebarose Juliyana, S.; Udaya Prakash, J. Optimisation of drilling process parameters of aluminium matrix composites (LM5/ZrO₂). *Int. J. Enterp. Netw. Manag.* **2023**, *14*, 193–204.
27. Juliyana, S.J.; Prakash, J.U. Optimization of burr height in drilling of aluminium matrix composites (LM5/ZrO₂) using Taguchi technique. *Adv. Mater. Process. Technol.* **2022**, *8*, 417–426. [[CrossRef](#)]
28. Juliyana, S.J.; Prakash, J.U. Drilling parameter optimization of metal matrix composites (LM5/ZrO₂) using Taguchi Technique. *Mater. Today Proc.* **2020**, *33*, 3046–3050. [[CrossRef](#)]
29. Gigan, S. Optical microscopy aims deep. *Nat. Photon.* **2017**, *11*, 14–16. [[CrossRef](#)]
30. Mertz, J. *Introduction to Optical Microscopy*, 2nd ed.; Cambridge University Press: Cambridge, UK, 2019. [[CrossRef](#)]
31. Azad, M.; Avin, A. Scanning Electron Microscopy (SEM): A Review. In Proceedings of the 2018 International Conference on Hydraulics and Pneumatics—HERVEX, Baile Govora, Romania, 7–9 November 2018; pp. 1–9.
32. Ouakki, M.; Galai, M.; Benzekri, Z.; Verma, C.; Ech-Chihbi, E.; Kaya, S.; Boukhris, S.; Ebenso, E.E.; Touhami, M.E.; Cherkaoui, M. Insights into corrosion inhibition mechanism of mild steel in 1 M HCl solution by quinoxaline derivatives: Electrochemical, SEM/EDAX, UV-visible, FT-IR and theoretical approaches. *Colloids Surfaces A Physicochem. Eng. Asp.* **2021**, *611*, 125810. [[CrossRef](#)]
33. Li, Y.; Kim, H.N.; Wu, H.; Kim, M.J.; Ko, J.W.; Park, Y.J.; Huang, Z.; Kim, H.D. Microstructure and thermal conductivity of gas-pressure-sintered Si₃N₄ ceramic: The effects of Y₂O₃ additive content. *J. Eur. Ceram. Soc.* **2021**, *41*, 274–283. [[CrossRef](#)]
34. Broitman, E. Indentation Hardness Measurements at Macro-, Micro-, and Nanoscale: A Critical Overview. *Tribol. Lett.* **2017**, *65*, 23. [[CrossRef](#)]
35. Rezayat, M.; Yazdi, M.S.; Zandi, M.D.; Azami, A. Tribological and corrosion performance of electrodeposited Ni-Fe/Al₂O₃ coating. *Results Surf. Interfaces* **2022**, *9*, 100083. [[CrossRef](#)]
36. Ashkani, O.; Tavighi, M.R.; Karamimoghadam, M.; Moradi, M.; Bodaghi, M.; Rezayat, M. Influence of Aluminum and Copper on Mechanical Properties of Biocompatible Ti-Mo Alloys: A Simulation-Based Investigation. *Micromachines* **2023**, *14*, 1081. [[CrossRef](#)]
37. Idrisi, A.H.; Mourad, A.-H.I. Conventional stir casting versus ultrasonic assisted stir casting process: Mechanical and physical characteristics of AMCs. *J. Alloys Compd.* **2019**, *805*, 502–508. [[CrossRef](#)]
38. Jiang, B.; Zhenglong, L.; Xi, C.; Peng, L.; Nannan, L.; Yanbin, C. Microstructure and mechanical properties of TiB₂-reinforced 7075 aluminum matrix composites fabricated by laser melting deposition. *Ceram. Int.* **2019**, *45*, 5680–5692. [[CrossRef](#)]
39. Sharma, D.K.; Sharma, M.; Upadhyay, G. Services, Boron Carbide (B₄C) Reinforced Aluminum Matrix Composites (AMCs). *Int. J. Innov. Technol. Explor. Eng.* **2019**, *9*, 2194–2203. [[CrossRef](#)]

40. Abdel Hakam, R.; Abdel Aziz Taha, M. Study of mechanical properties and wear behavior of nano-ZrO₂-hardened Al2024 matrix composites prepared by stir cast method. *Egypt. J. Chem.* **2022**, *65*, 307–313.
41. Udayashankar, S.; Ramamurthy, V.S. Development and Characterization of Al 6061-ZrO₂ Reinforced Metal Matrix Composites. *Int. J. Eng. Technol.* **2018**, *7*, 128–132.
42. Pai, B.C.; Ramani, G.; Pillai, R.M.; Satyanarayana, K.G. Role of magnesium in cast aluminium alloy matrix composites. *J. Mater. Sci.* **1995**, *30*, 1903–1911. [[CrossRef](#)]
43. Yar, A.A.; Montazerian, M.; Abdizadeh, H.; Baharvandi, H. Microstructure and mechanical properties of aluminum alloy matrix composite reinforced with nano-particle MgO. *J. Alloy Compd.* **2010**, *484*, 400–404. [[CrossRef](#)]
44. Prakash, J.U.; Juliyana, S.J.; Pallavi, P.; Moorthy, T. Optimization of Wire EDM Process Parameters for Machining Hybrid Composites (356/B4C/Fly Ash) using Taguchi Technique. *Mater. Today Proc.* **2018**, *5*, 7275–7283. [[CrossRef](#)]
45. Biswas, P.; Mandal, D.; Mondal, M.K. Failures analysis of in-situ Al–Mg₂Si composites using actual microstructure based model. *Mater. Sci. Eng. A* **2020**, *797*, 140155. [[CrossRef](#)]
46. Samal, P.; Vundavilli, P.R.; Meher, A.; Mahapatra, M.M. Recent progress in aluminum metal matrix composites: A review on processing, mechanical and wear properties. *J. Manuf. Process.* **2020**, *59*, 131–152. [[CrossRef](#)]
47. Abdizadeh, H.; Baghchesara, M.A. Investigation on mechanical properties and fracture behavior of A356 aluminum alloy based ZrO₂ particle reinforced metal-matrix composites. *Ceram. Int.* **2013**, *39*, 2045–2050. [[CrossRef](#)]
48. Al-Jaafari, M.A. A comparative study using silicon carbide and zirconium dioxide nano material's to improve the mechanical properties of 6261AA. *Period. Eng. Nat. Sci.* **2022**, *10*, 323–333.
49. Juliyana, S.J.; Prakash, J.U.; Salunkhe, S.; Hussein, H.M.A.; Gawade, S.R. Mechanical Characterization and Microstructural Analysis of Hybrid Composites (LM5/ZrO₂/Gr). *Crystals* **2022**, *12*, 1207. [[CrossRef](#)]
50. Vatin, N.I.; Murali, G.; Abid, S.R.; de Azevedo, A.R.G.; Tayeh, B.A.; Dixit, S. Enhancing the Impact Strength of Prepacked Aggregate Fibrous Concrete Using Asphalt-Coated Aggregates. *Materials* **2022**, *15*, 2598. [[CrossRef](#)]

Disclaimer/Publisher's Note: The statements, opinions and data contained in all publications are solely those of the individual author(s) and contributor(s) and not of MDPI and/or the editor(s). MDPI and/or the editor(s) disclaim responsibility for any injury to people or property resulting from any ideas, methods, instructions or products referred to in the content.